

# Closed-Form Solutions for Broad-Band Equivalent Circuit of Vertical Rod Buried in Lossy Grounds Subjected to Lightning Strokes

Ali Bagheri<sup>1</sup>, S. R. Ostadzadeh<sup>2</sup>, and M. Kazemi<sup>3</sup>

<sup>1</sup>Arak University, Faculty of engineering, BSC student, Arak38156-8-8349, Iran, Ali.Bag.73@gmail.com

<sup>2</sup>Arak University, Faculty of engineering, Assistant Professor, Arak38156-8-8349, Iran, s-ostadzadeh@araku.ac.ir

<sup>3</sup>Imam Khomeini Oil Refinery Company of Shazand, Arak, Iran, Kazemi\_elec@yahoo.com

Corresponding author: Saeed Reza Ostadzadeh

**Abstract**— In this paper, input impedance of a vertical rod under lightning stroke is first computed by applying the method of moments (MoM) on the Maxwell's equations. The circuit model is then achieved through applying modified vector fitting (MVF) on the computed input impedance. After then the equivalent circuit is again extracted for a few values of ground conductivity and rod radius. Finally using a new fuzzy-based model namely spatial membership functions, closed form solutions for all lumped elements of the equivalent circuit are achieved.

**Index Terms**— Closed-form, lossy ground, lightning stroke, vertical rod, MVF.

## I. INTRODUCTION

As known, when lightning strikes the overhead line towers or shielding wires directly, or indirectly, lightning current induced along overhead lines is injected to the tower footing. Lightning performance of overhead lines can be carried out via transient solvers such as ATP-EMTP [1], EMTP-RV [2], and PSCAD/EMTDC [3]. It is well known that EMTP models each system as equivalent circuit or transmission line. Therefore overhead lines, tower and grounding should be imported as equivalent circuit or transmission line.

Depending upon electrical parameters of ground are constant or frequency-dependent, overhead line in EMTP can be modeled as CP (constant parameters) or FD (frequency dependence) lines. Tower is also modelled as a resistor as explained in [4]. In the case of grounding system, however, EMTP models it either as lumped resistor or an equivalent circuit of the inductor, resistor and capacitor [5].

One of conventional grounding systems is vertical rod. Figure 1 shows schematic diagram of a vertical rod under lightning strike with different equivalent circuits. The values of lumped elements of equivalent circuits (R, L, and C) in figure 1 are as following:

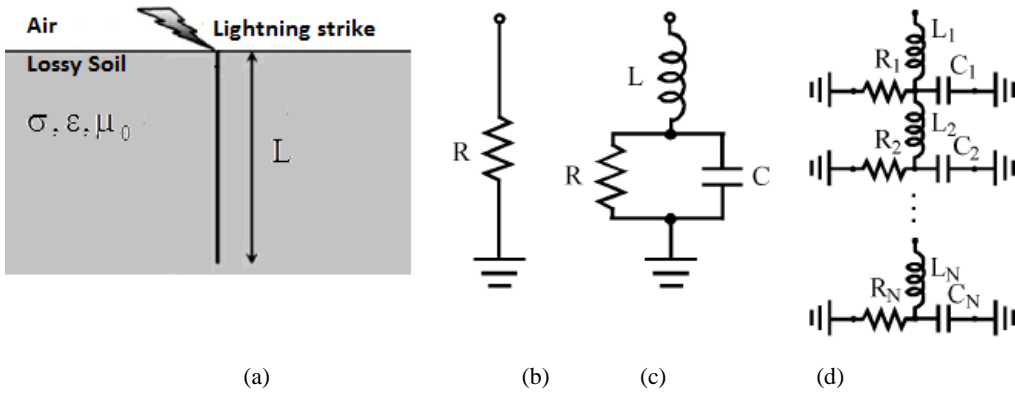


Fig. 1. (a) Schematic diagram of the vertical rod buried in dispersive lossy ground subjected to lightning strikes, (b) resistive model, (c) RLC model, (d): distributed RLC model. Adopted from [5].

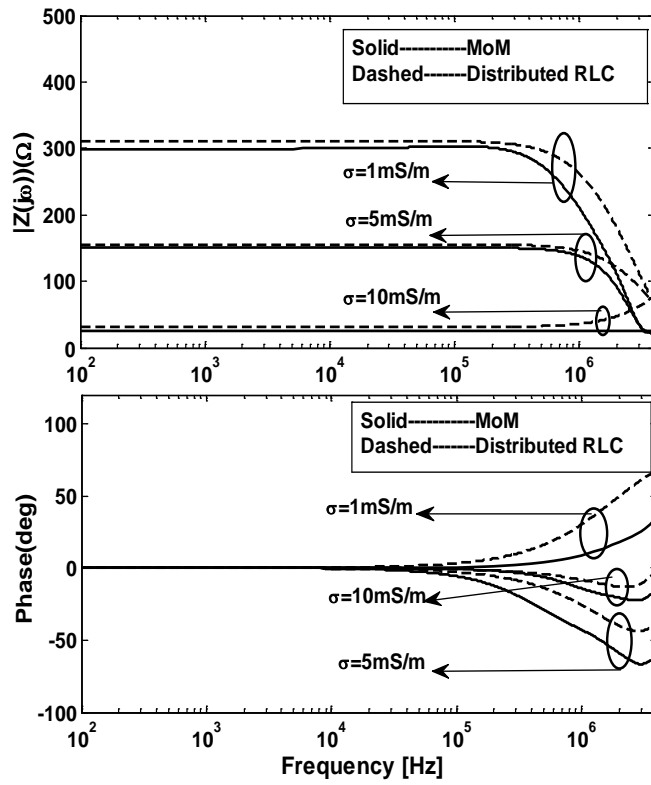


Fig. 2. Magnitude and phase of the input impedance of a vertical rod buried in lossy ground for three values of conductivity.

$$R = \frac{1}{2\pi l \sigma} \left[ \ln\left(\frac{4l}{a}\right) - 1 \right] (\Omega) \quad (1)$$

$$L = \frac{\mu_0 l}{2\pi} \left[ \ln\left(\frac{2l}{a}\right) - 1 \right] (\text{H}) \quad (2)$$

$$C = 2\pi \epsilon l / \left[ \ln\left(\frac{4l}{a}\right) - 1 \right] (\text{F}) \quad (3)$$

Since the lightning current injected to grounding systems includes wide-band frequency content from dc to a few MHz, the mentioned circuits which are based upon static or quasi-static assumptions are violated. For instance, figure 2 shows magnitude and phase of the input impedance of a vertical

rod of length 3m for a few values of ground conductivity. As seen in this figure, at high frequencies the distributed RLC is violated from accurate method of moments (MoM) [6].

More recently to introduce wide-band models a few attempts on equivalent circuit or transmission line model, have been carried out [7-9] and later a few models based upon frequency domain approaches such as modified vector fitting (MVF) [10-12] and matrix pencil method (MPM) have been proposed [13-15]. These approaches, however, suffer from time consuming and repetitive computations due to method of moments (MoM) at each frequency sample and instability problems of MVF and MPM. These drawbacks are repeated when weather conditions are changing, i.e., conductivity of ground is changing.

To the best our knowledge, there is no closed-form solution for wide-band models mentioned above. Hence in this study, MVF is first used to extract equivalent circuit of the vertical rod buried in lossy ground for a few values of ground conductivity and rod radius. Then based upon an efficient fuzzy model namely spatial membership functions [16], closed-form solutions for all elements of equivalent circuit are inferred.

This paper is organized as follows. In section 2, principles of the modeling process based upon membership functions are briefly explained. Section 3 is focused on extracting wide-band equivalent circuit of vertical rod using MVF and then inferring closed-form solutions. Finally conclusion is given in section 4.

## II. BASIC PRINCIPLES OF MODELING USING SPATIAL MEMBERSHIP FUNCTIONS

As known, there are different intelligent modeling approaches such as fuzzy inference models [17-19], and neural networks ones [20, 21], but when the number of inputs are increased due to training process, these models are inefficient and difficult. To remove these drawbacks, S. B. Shouraki et al [16, 22-24], proposed efficient approaches based upon fuzzy inference for multi-input, multi-output nonlinear systems. In the modeling approaches, at first, a nonlinear system of N inputs is divided into N single-input nonlinear systems, and then each of them are separately modeled by conventionally fuzzy-based models [17-19]. To achieve complete model, outputs of N systems are then combined through spatial membership functions (for systems of two inputs) [16] and active learning method (ALM) (for systems of more than two inputs) [22-24]. Since the nonlinear systems modeled in this study include only two inputs, hence in this study the modeling approach via the spatial membership functions is demonstrated.

Assume a nonlinear system of two inputs namely  $x_1, x_2$  and single output namely  $y$ . Let  $y_1$  to be the output of the same nonlinear system with single input  $x_1$  (when  $x_2$  is constant) and  $y_2$  to be the

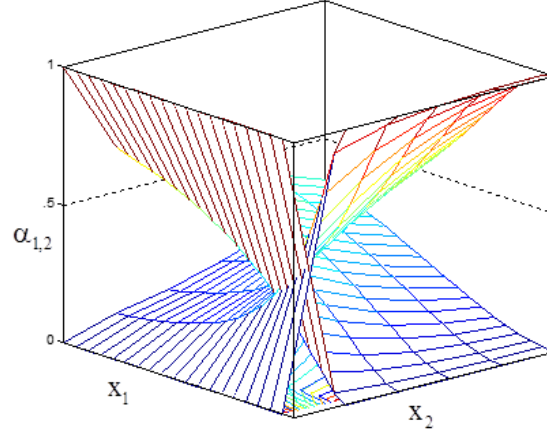


Fig 3. Two spatial membership functions for two independent variables under assumption of  $\beta_{1,2} = 1$ .

output of this nonlinear system with single input  $x_2$  (when  $x_1$  is constant). The output  $y$  when two inputs  $x_1$  and  $x_2$  are simultaneously changed is then inferred as following:

$$y = \frac{y_1\alpha_1 + y_2\alpha_2}{\alpha_1 + \alpha_2} \quad (4)$$

Where  $\alpha_1$  and  $\alpha_2$  are spatial membership functions and expressed as following:

$$\alpha_i(x_1, x_2) = \begin{cases} \frac{1}{2} \left( 1 - \cos \pi \left[ \frac{\Psi - \varphi_2}{\varphi_1 - \varphi_2} \right]^{\beta_1} \right) & \text{for } \Psi : \varphi_1 \rightarrow \varphi_2 \\ \frac{1}{2} \left( 1 + \cos \pi \left[ \frac{\Psi - \varphi_2}{\varphi_1 - \varphi_2} \right]^{\beta_2} \right) & \text{for } \Psi : \varphi_1 \rightarrow \varphi_2 \end{cases} \quad (5)$$

Where  $i = 1, 2$  and  $\psi = \tan^{-1}(x_2 / x_1)$ .

The two parameters  $\beta_1$  and  $\beta_2$  in (5) are for better prediction and optimized for an input-output sample. Figure 3 shows two spatial membership functions under assumption of  $\beta_{1,2} = 1$ . As shown in this figure, each spatial membership function has belongingness one on the individual axis and is decreasing to zero on the other axis. Further information in detail about modeling two-input nonlinear systems are in the next section. Recently use of the ALM has been proposed in designing microwave filters [22-24].

### III. CLOSED-FORM SOLUTIONS FOR EQUIVALENT CIRCUIT OF VERTICAL ROD

In this section, the vertical rod of length  $l = 3\text{m}$  and buried in lossy ground with relative dielectric constant  $\epsilon_r = 10$  and conductivity  $\sigma$  is considered. To extract equivalent circuit, the input impedance of the rod in the frequency domain is first computed by MoM and then through MVF, the input impedance is converted to rational functions, and finally equivalent circuit is easily achieved. Further information about this process is found in [10-12]. Hence in this section, closed-form solution for the

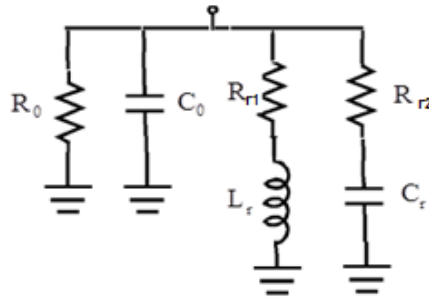
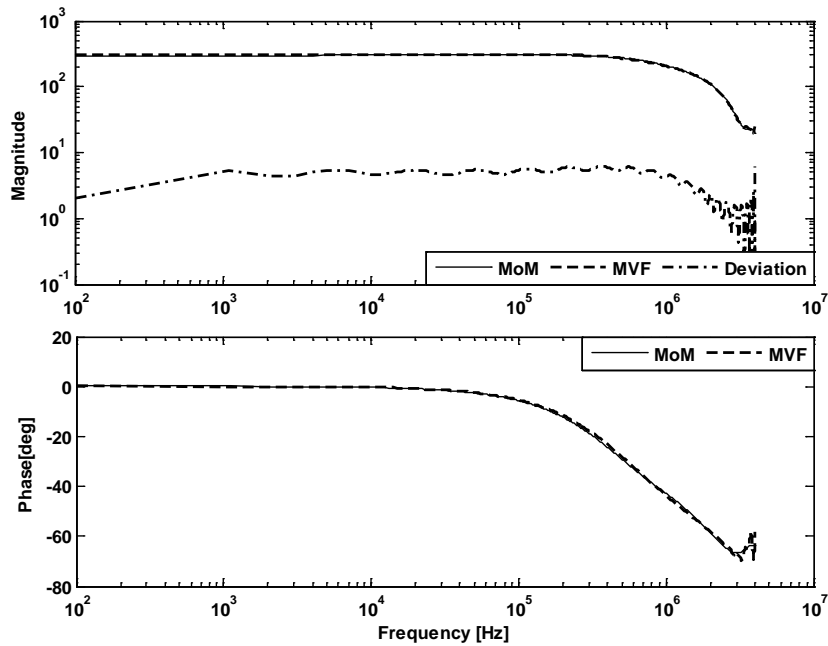
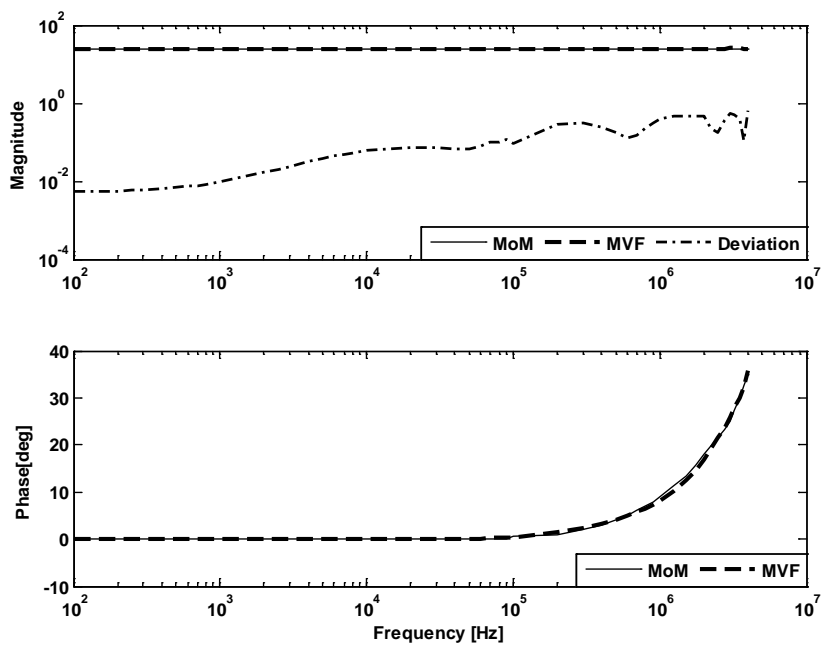


Fig. 4. Equivalent circuit extracted by MVF with two starting poles.



(a)



(b)

Fig. 5. Comparing the modelled input impedance via MVF and MOM for (a)  $\sigma = 1\text{mS/m}$  and (b)  $\sigma = 10\text{mS/m}$ .

each lumped element of equivalent circuit of the vertical rod is inferred. Under this assumption, the schematic diagram of equivalent circuit with two starting poles extracted by MVF is shown in the figure 4.

To know with two starting poles how accurate fitting is, figure 5 shows fitting the input impedance via MVF and compares with MoM for two values of conductivities.

For the vertical rod, two inputs, i.e., the radius of the rod or  $\Omega = \ln(2l/a)$  (a measure of radius) and ground conductivity,  $\sigma$ , in addition, 6 outputs (6 lumped elements in the equivalent circuit) are existed. Hence in the next sub-sections, effects of these inputs on the each output are separately extracted, and the simultaneous effects of them on the each output are then inferred. It should be noted that since the modelling process for each output is the same, hence for shortening the paper, closed-form solution only for two outputs of  $R_0$  and  $C_0$  are inferred.

#### A. Ground Conductivity Effect

Without losing generality among 6 elements of the equivalent circuit in the figure 4, fuzzy-based models for  $R_0$  and  $C_0$  versus input  $\sigma$  (as input), are only introduced. The other ones are similarly modeled. In the modeling process, MVF is first applied to the input impedance in the frequency range of [100Hz-4MHz] for a few values of  $\sigma = 1,5,9$  (mS/m) under assumption of  $\Omega=5$ . Assigning membership function or belongingness in this range for these samples is the second step. The membership functions here used are as following:

$$\alpha(\sigma) = \begin{cases} \frac{1}{2} \left(1 + \cos \pi \left(\frac{\sigma - a_1}{a_2 - a_1}\right)^{\beta_1}\right) & \sigma : a_1 \rightarrow a_2 \\ \frac{1}{2} \left(1 - \cos \pi \left(\frac{\sigma - a_1}{a_2 - a_1}\right)^{\beta_2}\right) & \sigma : a_1 \rightarrow a_2 \end{cases} \quad (6)$$

Here for each chosen sample  $\sigma$ , one membership function is used in such a way that for each  $\sigma$ , the individual membership function has belongingness one and is decreasing to zero on the neighbour  $\sigma$ 's. Also, in (6),  $a_1$  and  $a_2$  are boundary points in which membership functions have belongingness one or zero. Figure 6 shows three membership functions with belongingness between 0 to 1. From now on, for other values of  $\sigma$  without needing to the MoM and MVF,  $R_0$  and  $C_0$  are easily predicted by Takagi-Sugeno's technique [17] as follows:

$$\left\{ \begin{array}{l} R_0(\sigma) = \frac{\sum_{i=0}^3 R_{i\sigma} \alpha_i(\sigma)}{\sum_{i=1}^3 \alpha_i(\sigma)} \\ C_0(\sigma) = \frac{\sum_{i=0}^3 C_{i\sigma} \alpha_i(\sigma)}{\sum_{i=1}^3 \alpha_i(\sigma)} \end{array} \right. \quad (7)$$

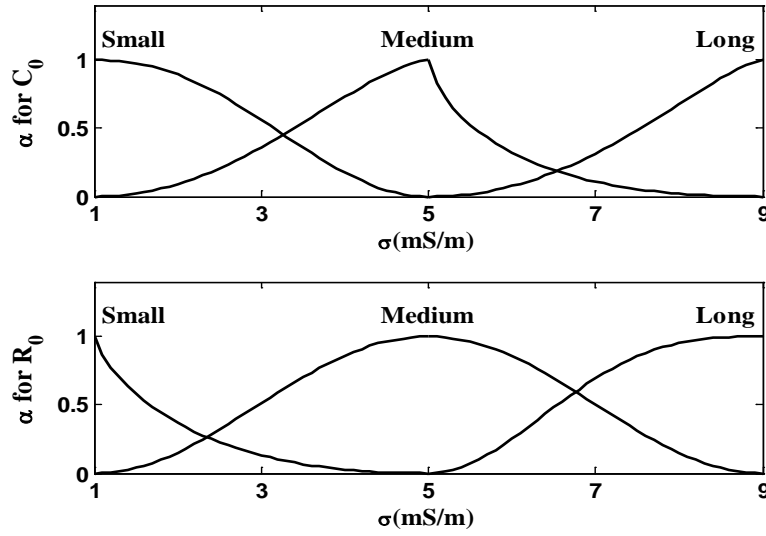


Fig. 6. The membership function of  $R_0$  and  $C_0$  versus input  $\sigma$ .

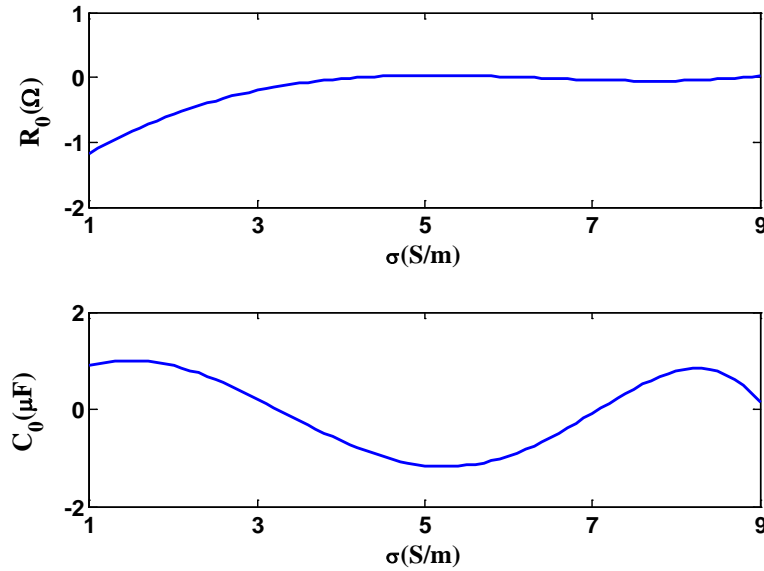


Fig. 7. Prediction of  $R_0$  and  $C_0$  versus input  $\sigma$  via the proposed model.

Where  $R_{i\sigma}$  and  $C_{i\sigma}$  are the values of  $R_0$  and  $C_0$  extracted by MVF for samples  $\sigma = 1,5,9(\text{mS}/\text{m})$ . Also  $\alpha_i, i = 1,2,3$  are membership functions for the three samples as shown in figure 6.

For accurate prediction, the above membership functions are optimized through adjusting  $\beta_1$  and  $\beta_2$  in (6) for two samples  $\sigma = 3,7(\text{mS}/\text{m})$ . The optimum membership functions are shown in figure 6. Figure 7 shows the predicted curves of  $R_0$  and  $C_0$  versus  $\sigma$ .

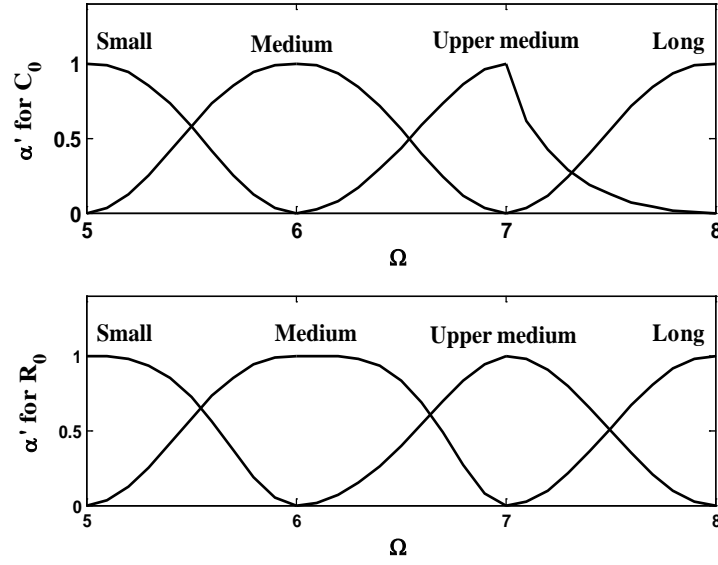


Fig 8. The optimum membership functions of  $R_0$  and  $C_0$  versus input  $\Omega$ .

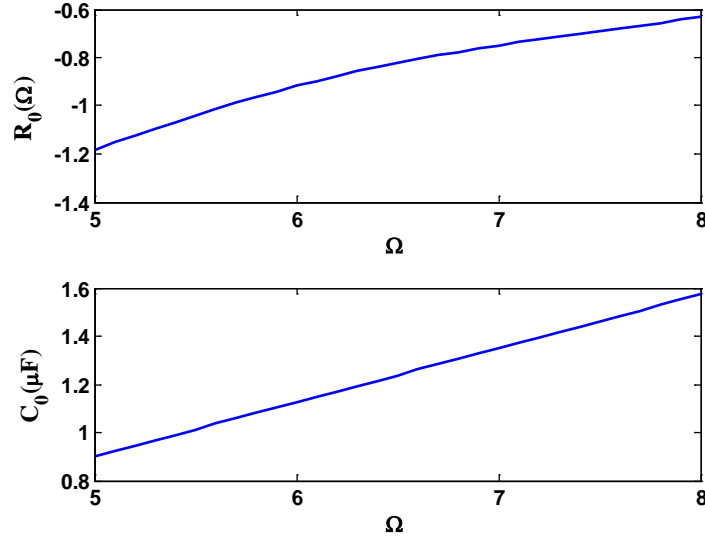


Fig. 9. Prediction of  $R_0$  and  $C_0$  versus input  $\Omega$  by the proposed model.

### B. Rod Radius Effect

In this sub section, the same as previous one, fuzzy-based models for  $R_0$  and  $C_0$  versus input  $\Omega$  are proposed. Hence MVF is first applied to the input impedance in the frequency range of [100Hz-4MHz] for a few values of  $\Omega = 5, 6, 7, 8$  under assumption of  $\sigma = 1\text{mS/m}$ . The expression for membership functions and the Takagi-Surgeon's equations are as follows:

$$\alpha(\Omega) = \begin{cases} \frac{1}{2} \left( 1 + \cos \pi \left( \frac{\Omega - a_1}{a_2 - a_1} \right)^{\beta_1} \right) & \Omega : a_1 \rightarrow a_2 \\ \frac{1}{2} \left( 1 - \cos \pi \left( \frac{\Omega - a_1}{a_2 - a_1} \right)^{\beta_2} \right) & \Omega : a_1 \rightarrow a_2 \end{cases} \quad (8)$$

$$\left\{ \begin{array}{l} R_0(\Omega) = \frac{\sum_{i=0}^4 R_{i\Omega} \alpha'_i(\Omega)}{\sum_{i=1}^4 \alpha'_i(\Omega)} \\ C_0(\Omega) = \frac{\sum_{i=0}^4 C_{i\Omega} \alpha'_i(\Omega)}{\sum_{i=1}^4 \alpha'_i(\Omega)} \end{array} \right. \quad (9)$$

Where  $R_{i\Omega}$  and  $C_{i\Omega}$  are the values of  $R_0$  and  $C_0$  extracted by MVF for samples  $\Omega = 5,6,7,8$  under assumption of  $\sigma = 1\text{mS/m}$ . In addition,  $\alpha'_i, i = 1,2,3$  are membership functions for the three samples as shown in figure 8. Finally figure 9 shows predicted curves of  $R_0$  and  $C_0$  versus  $\Omega$  through the proposed model.

### C. Complete Model

In the two previous sections, single-input fuzzy models for  $R_0$  and  $C_0$  were extracted. To include the simultaneous effects of two inputs on  $R_0$  and  $C_0$ , the spatial membership functions of the following forms are used.

$$\alpha_i(\Omega, \sigma) = \begin{cases} \frac{1}{2} \left( 1 - \cos \pi \left[ \frac{\varphi - \varphi_2}{\varphi_1 - \varphi_2} \right]^{\beta_1} \right) & \text{for } \varphi : \varphi_1 \rightarrow \varphi_2 \\ \frac{1}{2} \left( 1 + \cos \pi \left[ \frac{\varphi - \varphi_2}{\varphi_1 - \varphi_2} \right]^{\beta_2} \right) & \text{for } \varphi : \varphi_1 \rightarrow \varphi_2 \end{cases} \quad (10)$$

in which  $\varphi = \tan^{-1}(\frac{\Omega}{\sigma_n})$ , Also  $\sigma_n$  is normalized conductivity ( $\sigma_n = \sigma/0.001$ ). The following inference equations which are in the general form of Takagi-Surgeon's technique can now be used to extract  $R_0$  and  $C_0$  versus  $\Omega$  and  $\sigma$  simultaneously.

$$R_0(\Omega, \sigma) = \frac{R_0(\Omega)\alpha_1(\Omega, \sigma) + R_0(\sigma)\alpha_2(\Omega, \sigma)}{\alpha_1(\Omega, \sigma) + \alpha_2(\Omega, \sigma)} \quad (11-a)$$

$$C_0(\Omega, \sigma) = \frac{C_0(\Omega)\alpha'_1(\Omega, \sigma) + C_0(\sigma)\alpha'_2(\Omega, \sigma)}{\alpha'_1(\Omega, \sigma) + \alpha'_2(\Omega, \sigma)} \quad (11-b)$$

Where  $\alpha_{1,2}$  and  $\alpha'_{1,2}$  are spatial membership functions for linguistic modeling  $R_0$  and  $C_0$  versus the two inputs as shown in figure 10 and 11 respectively.

In these figures, two fuzzy sets for two independent inputs  $(\Omega, \sigma)$  are seen. Each fuzzy set has belongingness value of one on its individual axis and is smoothly decreasing to zero on the other axis. To extract  $R_0$  and  $C_0$  accurately,  $\beta_1$  and  $\beta_2$  in (10) are optimized for sample  $\Omega=5.5$  and

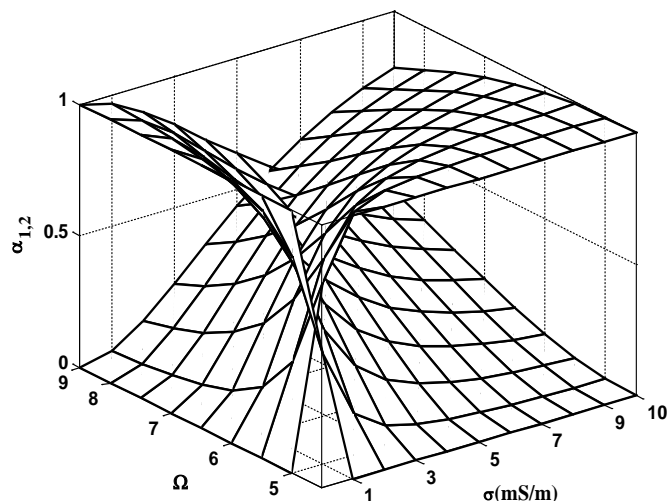


Fig. 10. Optimum spatial membership functions  $\alpha_{1,2}$  for combining effects of  $\Omega$  and  $\sigma$  on  $R_0$ .

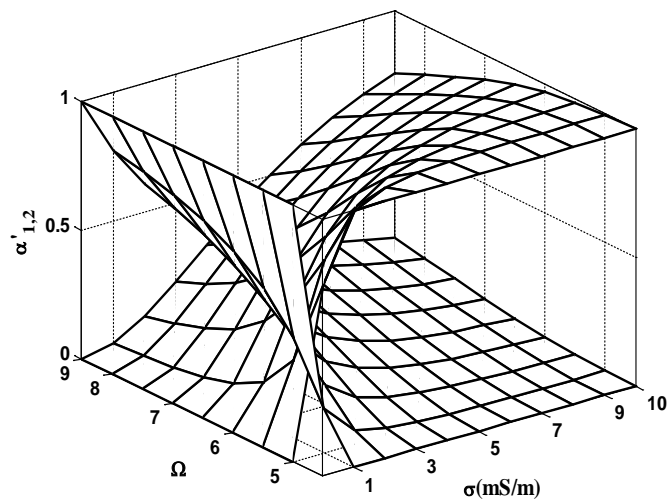


Fig. 11. Optimum spatial membership functions  $\alpha'_{1,2}$  for combining effects of  $\Omega$  and  $\sigma$  on  $C_0$ .

$\sigma = 2\text{mS/m}$ . The variation of  $C_0$  and  $R_0$  versus two inputs  $\Omega$  and  $\sigma$  are shown in figure 12 and 13 respectively.

To know how accurate the achieved models are, the predicted values for  $C_0$  and  $R_0$  by the proposed models and the MVF are compared as shown in figures 14 and 15 respectively. As it is seen in these figures, excellent agreement is achieved. Now using the inferred values for lumped elements, the equivalent circuit for arbitrary sample is easily extracted. Figure 16 shows the extracted equivalent circuit when  $\sigma = 5\text{mS/m}$  and  $\Omega = 6$ . In this figure, resistors, inductors, and capacitances are in Ohm, Henry and Farad.

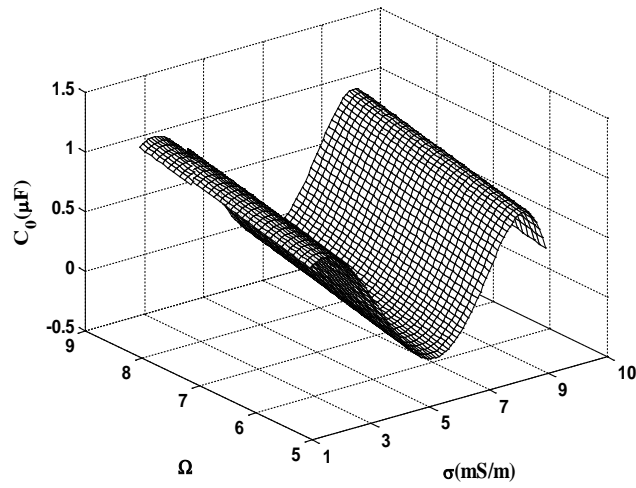


Fig. 12. Variation of  $C_0$  versus two independent inputs ( $\Omega, \sigma$ ).

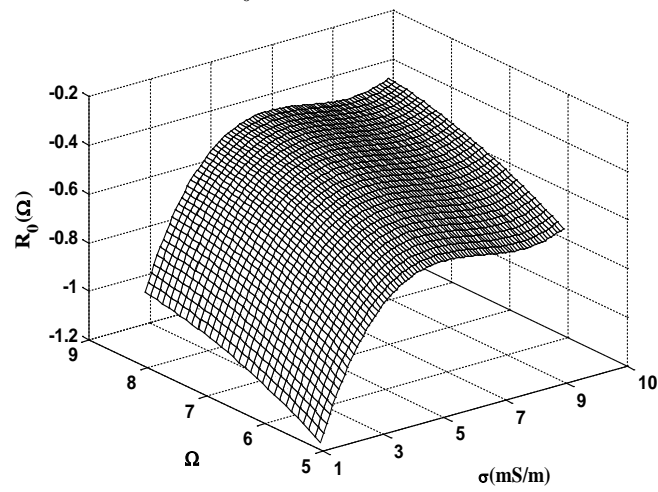


Fig. 13. Variation of  $R_0$  versus two independent inputs ( $\Omega, \sigma$ ).

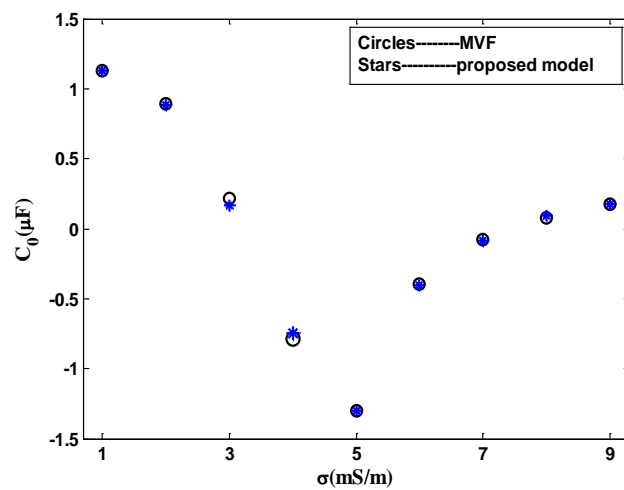


Fig. 14. Comparison of the predicted value of  $C_0$  when  $\sigma$  is variable and  $\Omega=6$  with MVF.

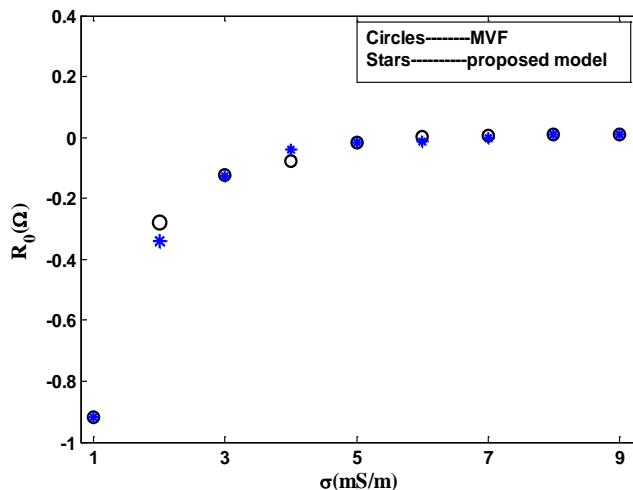


Fig. 15. Comparison of the predicted value of  $R_0$  when  $\sigma$  is variable and  $\Omega=6$  with MVF.

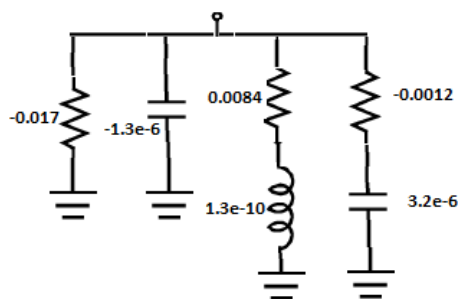


Fig. 16. Inferred equivalent circuit through the proposed model when  $\sigma = 5\text{mS/m}$  and  $\Omega = 6$ .

#### IV. CONCLUSION

In this paper, assuming the ground as a lossy medium, wide-band equivalent circuit of a vertical rod with simple formulae were inferred for the first time. In extracting these formulae, MVF was first applied to the input impedance of the rod in the frequency domain, and the equivalent circuits for a few values of ground conductivity and rod radius were then extracted. After then based upon spatial membership functions, fuzzy model for each element of equivalent circuit is easily achieved. As a result, these values can be interfaced with transient solvers in transient analyses of power systems accurately. In extracting equivalent circuit, two starting poles were extracted.

It is evident that choosing more starting poles results to more accurate equivalent circuit. Inferring closed-form solutions for vertical rod buried in lossy dispersive ground (electrical parameters of ground are frequency dependent) can be similarly carried out.

#### REFERENCES

- [1] Alternative Transients Program (ATP): Rule Book, Can./Amer. EMTP User Group, Leuven EMTP Center, Leuven, Belgium, 1987.
- [2] J. Mahseredjian, S. Denetiere, L. Dube, "On a new Approach for the Simulation of Transients in Power Systems," *Electr. Power Syst. Res.*, vol. 77, no. 11, pp. 1514-1520, 2007.

- [3] PSCAD/EMTDC User's Manual, ver. 42., Manitoba HVDC Res. Center, Winnipeg, MB, Canada, 2005.
- [4] T. Hara and O. Yamamoto, "Modelling of a Transmission Tower for Lightning-Surge Analysis," *IEE Proc. Gener. Transmiss. Distrib.*, vol. 143, no. 3, pp. 283-289, 1996.
- [5] Leonid Grcev, and Marjan Popov, "On High-Frequency Circuit Equivalents of a Vertical Ground Rod," *IEEE Trans. Power Del.*, vol. 20, no. 2, April 2005.
- [6] R.F. Harrington, *Field Computation by Moment Methods*, Macmillan, New York, 1968.
- [7] Leonid Grcev, "Modeling of Grounding Electrodes under Lightning Currents," *IEEE Trans. Electromagn. Compat.*, vol. 51, no. 3, August 2009.
- [8] Rajeev Thottappillil, "An Improved Transmission-Line Model of Grounding System," *IEEE Trans. Electromagn. Compat.*, vol. 43, no. 3, Aug 2001.
- [9] Yaqing. Liu, Yaqing Liul, "An Engineering Model for Transient Analysis of Grounding System Under Lightning Strikes: Non-uniform Transmission-Line Approach," *IEEE Trans. Power Del.*, vol. 20, no. 2, pp. 722-730, April 2005.
- [10] Bjorn Gustavsen, and Adam Semlyen, "Rational Approximation of Frequency Domain Responses By Vector Fitting", *IEEE Transaction on Power Delivery*, vol. 14, no. 3, pp. 517-524, 1999.
- [11] Bjorn Gustavsen, "Improving the Pole Relocating Properties of Vector Fitting", *IEEE Transaction on Power Delivery*, vol. 21, no. 3, 2006.
- [12] Bjorn Gustavsen, and Adam Semlyen, "Enforce Passivity for Admittance Matrices Approximated By Rational Functions", *IEEE Transaction on Power Delivery*, vol. 16, no. 1, 2001.
- [13] K. Sheshyekani, H. R. Karami, "Application of Matrix Pencil Method to Rational Fitting of Frequency-Domain Responses", *IEEE Transaction on Power Delivery*, vol. 27, no. 4, 2012.
- [14] K. Sheshyekani, M. R. Alemi, "Wide-Band Modeling of Large Grounding Systems to Interface with Electromagnetic Transient Solvers", *IEEE Transaction on Power Delivery*, vol. 29, no. 4, pp. 1868-1876, 2014.
- [15] K. Sheshyekani, M. Akbari, "Wide-Band Modeling of Tower-Footing Grounding Systems for the Evaluation of Lightning Performance of Transmission Lines", *IEEE Transaction on Power Delivery*, vol. 29, no. 4, 2015.
- [16] S. B. Shouraki, N. Honda "Fuzzy Prediction; A Method for Adaption," *14th fuzzy Symposium*, Gifu, Japan, pp.317-320, 2000.
- [17] Takagi, T. and M. Sugeno, "Fuzzy Identification of Systems and its Application to Modeling and Control," *IEEE Trans. on Systems, Man, and Cybernetics*, vol. SMC-15, no. 1, 1985.
- [18] Li-Xin Wang, "Generating Fuzzy Rules by Learning from Examples," *IEEE Trans on Systems, Man and Cybernetics*, vol. 22, 1992.
- [19] Michio Sugeno and Takahiro Yasukawa, "A Fuzzy-Logic-Based Approach to Qualitative Modeling," *IEEE Trans on Fuzzy Systems*, vol. 1, no. 1, 1993.
- [20] Q. J. Zhang and K. C. Gupta, *Neural Networks for RF and Microwave Design*. Boston, MA: Artech House, 2000.
- [21] C. Christodoulous and M. Georgiopoulos, *Applications of Neural Networks in Electromagnetics*. Boston, MA: Artech House, 2001.
- [22] Shouraki, S. B., Honda, N. "Recursive fuzzy modeling based on fuzzy interpolation", *Journal of Advanced Computational Intelligence*, vol. 3, no. 2, pp. 114 – 125, 1999.
- [23] P. Rezaee, M. Tayarani, "Active Learning Method for the Determination of the Coupling Factor and External Q in Microstrip Filter Design", *Progress in Electromagnetics Research*, vol. 120, pp. 459-479, 2011.
- [24] P. Rezaee, M. Tayarani, "Miniaturized Microstrip Design using Active Learning Method", *Radio Engineering*, vol. 18, no.1, pp. 259-4268, 2009.